

EXPERIMENTAL INVESTIGATIONS OF SHOCK WAVE PROPAGATION IN THE POSTFOCAL REGION OF A FOCUSED SOUND FIELD

H. HOBÆK

Department of Physics
University of Bergen
Allég. 55, N5007 Bergen, Norway

This paper reports some experimental results on the postfocal region of the sound field from a curved circular transducer at very high amplitude. It is found that along the axis the shock front seems to propagate with a speed different from the "background sound". This is explained by diffraction: The field may be separated into two main contributions, one from the edge of the source — arriving first and causing the "background sound" — and one from the main region of the source — causing the shock. After being formed the shock propagates with no change in shape, and with uniformly decreasing amplitude. The shock propagation speed seems to increase slightly with source amplitude.

1. Introduction

Focused ultrasound has many applications, as for example in medical diagnostics and therapy. The linear (small amplitude) field from focusing transducers is well known [1, 2], in particular if the parabolic wave equation is valid (i.e. if focusing angles $< 16^\circ$). Also the large amplitude case has received much attention lately [3, 4]. In this paper results from an experiment investigating the waveform in the post focal region are reported, and some of the findings seem not to have been published previously. In particular, it is found that the shock front, after being formed close to the focus, propagate along the axis with almost unaltered form but varying amplitude throughout the field, superposed a "background field" which seems to propagate with a different velocity. This is seen by recording time series of the waveform (traces) at increasing distances along the sound axis, in such a way that the traces display sequences in retarded time. In fact, the shock seems to be overtaken by the "sinusoidal" background field. Moreover it is found that beyond the focal region the arrival time of the shock depends on the source amplitude, even if the sound pulse (burst) contains many periods. Such behaviour is expected from single sound pulses, or if there is significant asymmetry in the signal (positive sound pressure peak exceeds that of the negative).

2. Experiment

A layout of the experimental arrangement is shown in Fig. 1, and the experimental parameters presented in Table 1. The source transducer was a circular cross section of a piezoelectric shell, with a fundamental resonance frequency about 1 MHz. Its radius of curvature was measured with a curvature gauge to 99 ± 2 mm. It was powered by a ENI 210L power amplifier through an impedance matching transformer, resulting in a maximum voltage of 370 V peak-to-peak measured at its terminals. Signals were

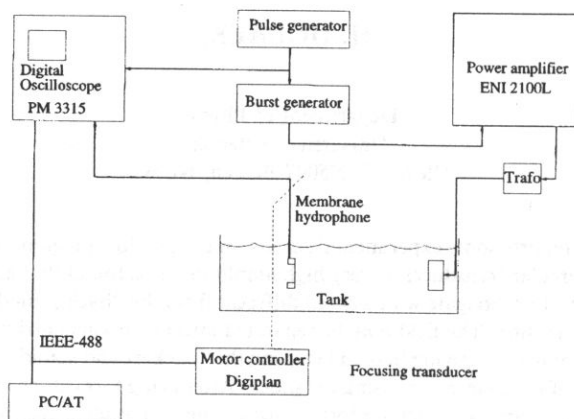


Fig. 1. Experimental arrangement.

Table 1. Experimental parameters

Tank dmensions:	
Length:	1.3 m
Width:	0.3 m
Height:	0.3 m
Contents:	Tap water, ca. 21°C
Sound speed:	1485 m/s
Focusing source:	
Radius of curvature:	99 ± 2 mm
Diameter:	47.85 mm
Frequency:	1.05 MHz
Wavelength:	1.41 mm
ka:	105.8
Rayleigh distance:	1.275 m
Length of near field:	405 mm
Gain-factor:	12.9
Focusing angle:	14°
Hydrophone:	
Diameter:	10 cm
Active surface:	1 mm diameter
Sensitivity (1 MHz):	0.155 mV/Pa

provided by a pulse generator delivering trigger signals to a bursts generator and the digital sampling oscilloscope (DSO). A jitter of up to $0.02\ \mu\text{s}$ from trace to trace was impossible to remove. The hydrophone was a bilaminar PVDF membrane type, with circular active area of 1 mm diameter. Its frequency response is reasonable flat to about 22 MHz. It was connected directly to the DSO through a 73 cm long $75\ \Omega$ cable. The DSO used for digitizing the signals was a PM 3315 (256 samples and up to 125 MHz sampling frequency with 8 bits resolution). The DSO and the positioning system was controlled by a PC/AT by IEEE-488 bus, and the records were transferred to the PC/AT for storage and further processing. The waveforms presented here (traces) are taken at the axis of the transducer, obtained by careful alignment of the source and hydrophone.

The burst used in this experiment were $125\ \mu\text{s}$ long. At the longest ranges this may have caused some interference from surface reflections in the weak parts of the signal, but this is believed not to have influenced the shock regions. The single traces were recorded in the following manner: after positioning the hydrophone at a new axial range, the first arrival of the burst was searched for the first clearly visible zero crossing in the positive direction. This was easily identifiable in all cases, and was used as a reference time for the trigger. To this was added the fixed delay of $100\ \mu\text{s}$. Thus, the traces always start $100\ \mu\text{s}$ after the first arrival of the burst.

3. Results

Figure 2 a–c show samples of traces taken at different ranges along the axis, with 370 V peak-to-peak driving voltage. Figure 2a shows three traces near the focal region. Note that there is no sign of a shock wave in the trace at 84 mm, which is just before the focus. The peak positive pressure of 2.08 V at 104 mm corresponds to 12.7 MPa, according to the nominal sensitivity of the hydrophone, while the peak negative pressure corresponds to $-2.8\ \text{MPa}$. Already at 124 mm the shock front is seen to be retarded significantly. The fluctuations just behind the shock front was thought to be due to the limited bandwidth of the hydrophone.

Figure 2b shows traces near the first axial zero outside the focal region, which is located at 194 mm as shown in Fig. 4. It is clearly seen how the shock arrives later as range increases, with respect to the “sinusoidal” background signal which remains stationary in the retarded frame.

Figure 2c shows samples of traces at longer ranges, in 80 mm steps. The shock front continues to arrive at later times relative to the sinusoidal background signal, although more and more slowly with increasing range. Observe that the shape of the shock front remains almost unchanged over the whole range, even through the axial zero at 194 mm. The rise time increases from $0.06\ \mu\text{s}$ to $0.08\ \mu\text{s}$ from 104 mm to 464 mm — although the amplitude varies strongly.

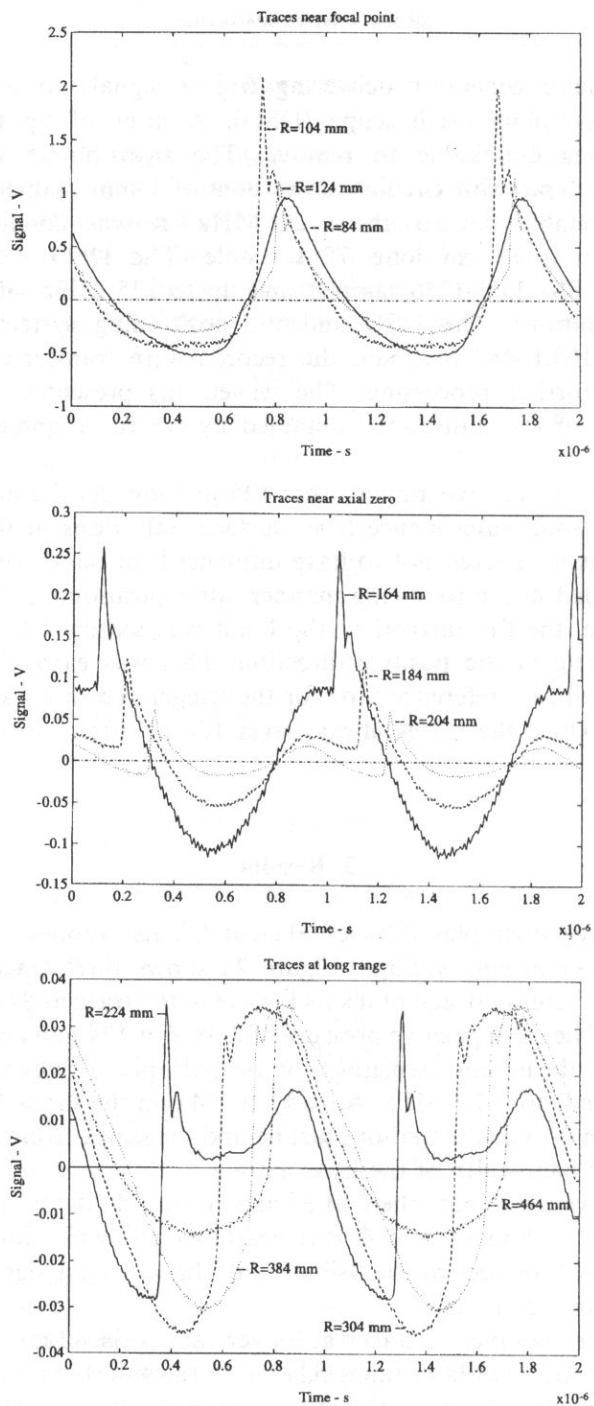


Fig. 2. Traces and different ranges.

Figure 3 shows amplitude variation with range, and the small amplitude simulations for this case (with arbitrary amplitude normalization). The shock amplitude is obtained by fitting a straight line to the shock front and taking the common part. It exceeds the positive peak amplitude when it starts below zero level, even in cases where the positive peak is higher than the peak of the shock. Where it is less than the positive peak the shock starts at a positive level. It is interesting to note that the negative peak amplitude has a minimum close to 200 mm, and another one about 470 mm, while that of the positive peak amplitude is at about 250 mm. The shock amplitude decreases uniformly with distance, although fastest within the first 100 mm

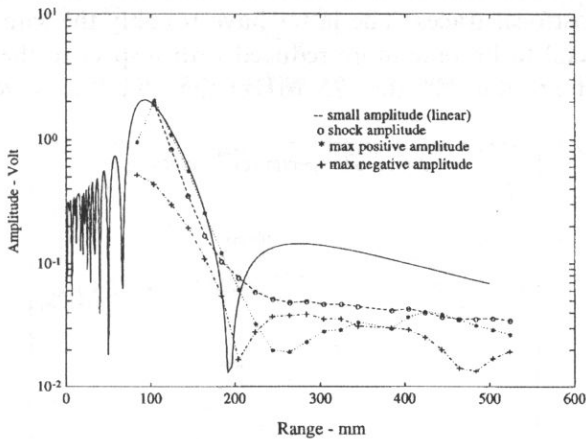


Fig. 3. Amplitude versus range.

front the focal region.

Figure 4 shows arrival times of the shock front and location of the positive and negative peak amplitudes, scaled in periods of the fundamental frequency. Also

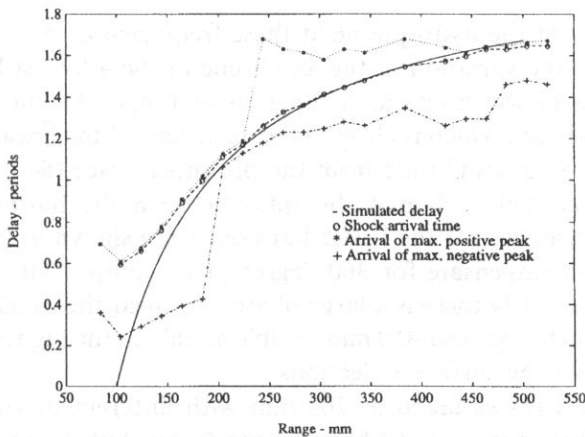


Fig. 4. Arrival times versus range.

shown is a curve representing the delay between arrivals of the wave from the edge of the source and that from the source center. The origin of the measured arrival times are adjusted so that the curve for the shock front coincides with the simulations at 384 mm. Jumps in the peak arrivals occur when the shock is overtaken by the background signal. Note that apart from these jumps the arrival times for the positive and negative peak amplitudes remain roughly constant (except where the positive peak coincides with the shock).

Figure 5 show amplitude spectra for the ranges 84–164 mm, up to the 26th harmonics. The amplitude at the fundamental frequency has been normalized to 1 in all the curves. There is, as expected, a major difference between the spectra of the prefocal and the postfocal traces. The latter have roughly the same shape, but the higher harmonics tend to become more reduced with respect to the fundamental as range increases. Above the 24th (i.e. 25 MHz) the amplitudes decay due to the

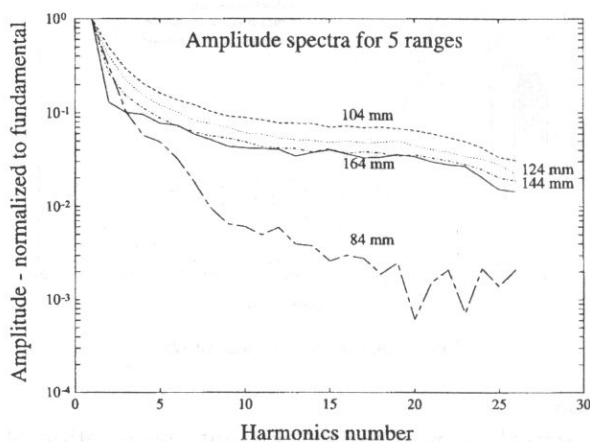


Fig. 5. Amplitude spectra for the ranges 84–164 mm, in 20 mm steps.

vanishing sensitivity of the hydrophone at these frequencies.

Figure 6a shows the variation of the amplitude of the 4 lowest harmonics in the frequency spectrum of the traces as a function of range. All the harmonics have a minimum near 204 mm, which is close to the axial zero of the linear field. Also note the change in harmonics amplitude from the pre-shock trace (84 mm) to the shock region. In the range 250–450 mm the ratio between the harmonics is roughly constant. The phase angles for the first 5 harmonics are shown in Fig. 6b. Attempts have been made to compensate for 360 degree phase jumps, but ambiguity in this respect remains. Obviously there is a large phase-shift near the axial zero at 194 mm, and another smaller change near 450 mm, visible mainly in the higher harmonics. The latter could be caused by surface reflections.

Figure 7 shows 3 traces taken at 202 mm with different driving voltages. The oscilloscope delay was not adjusted between the traces, but it was slightly different from the traces above. No shock exists in the trace at 138 V, and it is visible but not

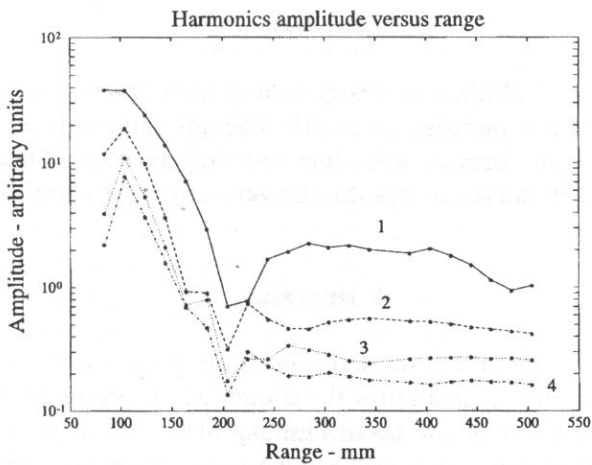


Fig. 6a. Variation of the amplitude of 1–4 harmonics with range.

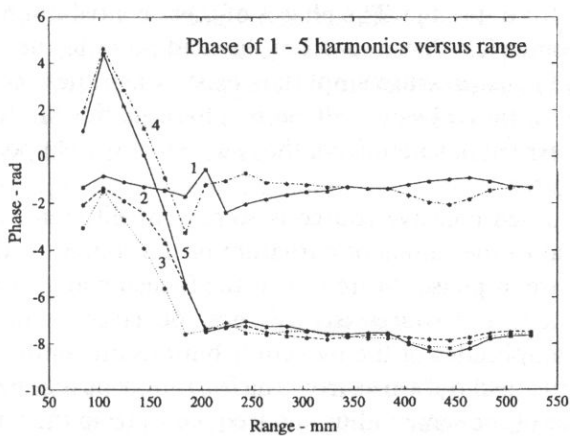


Fig. 6b. Variation of the phase angle of 1–5 harmonics with range.

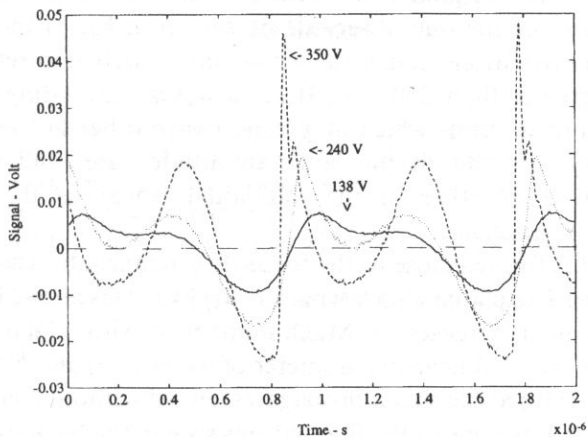


Fig. 7. Traces at 202 mm with different source amplitudes.

fully developed at 240 V. Still, it is clearly seen in these traces that the shock arrives earlier as the amplitude is increased, while the background signal, although not quite stationary and changing form as well, does not shift as much. This can be seen for example by shifting all curves so that falling zero crossings coincide.

4. Discussion

In order to explain the shift of the shock position relative to the background signal it is necessary to examine in detail how the sound field is produced. Here it is helpful to start with a discussion of the more familiar field from a plane circular piston source, in the linear regime. As is well known from elementary textbooks the axial field consists of two contributions of equal amplitude, namely one from the center of the source, and one from its edge. The phases of these contributions are proportional to the respective geometrical distances from the field point to these source points. In the near field zeros in the pressure amplitude exists when these contributions are in opposite phase, while they always will be in phase in the far field (on the axis). Obviously, the first arrival of sound from the source to any field point has its origin at the center of the source.

The field of a curved concave source is somewhat different. At the focal point — i.e. at range equal to the radius of curvature of the source — the central and the edge contributions are in phase. Moreover, if the focusing angle (angle between axis and line through focus and source edge) is not too large — in practice less than approx. 16° — the amplitudes of the two contributions are almost equal [5]. (It may also be shown that the field outwards from the focus may be mapped to the field from a plane piston source of the same radius and frequency, from the far field and inwards [6]). Outside the focus the first arrival of the signal will come from the edge of the source. Thus, if the shock originates from the central region of the source one should expect a retardation like the one observed. As shown in Fig. 4 the simulated delay between the two contributions match the actual shock arrival in retarded time quite nicely for ranges greater than 230 mm. It is, however, interesting to note that the central and edge contributions which may cancel each other in the small amplitude case, becomes very different in the large amplitude case, and actually may be distinguished from each other in the individual traces as the shock and the background signal respectively.

The shock itself is formed close to the focus. It is remarkable that it is not formed nearer to the source: The planar shock length $L = (\beta M k)^{-1}$ is about 14 cm in this case, but the converging field increases the Mach number M with a factor of almost 13 at the focus. Here β is the nonlinearity parameter of water (3.5) and k the wave number. However, after it is formed the shock propagates almost without change in shape. The shock amplitude exhibits none of the fluctuations seen in the background field, and in the harmonics. This is especially surprising with regard to the region around the axial zero (linear), where in the linear case a phase reversal takes place. The change in shock

arrival time with amplitude is explained by a well known result from weak shock theory, which is that the shock speed is the arithmetic mean of the speed just in front of the shock front, and the speed just behind it. Thus, if the waveform is highly asymmetric, as in the present investigation, the speed of the shock front is different from the small amplitude sound speed, and will depend on the amount of asymmetry. This asymmetry must be amplitude dependent (it appears only at high amplitudes) and has been seen by many previous investigators. The crucial question then remains: What is the physical explanation for this asymmetry?

5. Conclusions

The observed shock retardation with range is largely explained by accounting for the first arrival of sound as coming from the edge of the source. The shape of the shock itself remains remarkably stable throughout the post-focal zone, and its amplitude decays uniformly with range without fluctuations and phase reversal. It is, however, superimposed a background field originating from the source edge which is largely of the same amplitude, but contains no shocks. The shock seems to propagate with a speed which depends on the source amplitude. This is in accordance with weak shock theory.

Acknowledgments

The experiments were conducted during my sabbatical term visiting at School of Physics, University of Bath, England, whose hospitality is greatly acknowledged.

References

- [1] H.T. O'NEIL, J. Acoust. Soc. Am., **21**, 516 (1949).
- [2] B.G. LUCAS and T.G. MUIR, J. Acoust. Soc. Am., **72**, 1289 (1982).
- [3] A.C. BAKER, V.F. HUMPHREY and K. ANASTASIADIS, J. Acoust. Soc. Am., **84**, 1483 (1988).
- [4] S. NACHEF, *Générateur piezoelectrique d'ondes de choc a focalisation electronique*, Doctoral thesis, Institut national des sciences appliquées de Lyon 1992.
- [5] J. NAZE TJOTTA and S. TJOTTA, [in:] Frontiers of Nonlinear Acoustics [Ed.] M. Hamilton and D.T. Blackstock, Elsevier, London 1990, pp. 80.
- [6] H. HOBBAEK, [in:] Ultrasonics International Conference Proceedings, 1981, pp. 123.